

# Preferential melt intercalation of clay in ABS/brominated epoxy resin–antimony oxide (BER–AO) nanocomposites and its synergistic effect on thermal degradation and combustion behavior

Haiyun Ma, Zhengping Fang\*, Lifang Tong

*Institute of Polymer Composites, Zhejiang University, Hangzhou 310027, PR China*

Received 12 January 2006; received in revised form 15 February 2006; accepted 21 February 2006

Available online 18 April 2006

## Abstract

ABS/organo montmorillonite (OMT) nanocomposites and ABS/brominated epoxy resin–antimony oxide (BER–AO)/OMT nanocomposites were prepared via melt compounding. The dispersion of OMT in nanocomposites was investigated by wide-angle X-ray diffraction and transmission electron microscopy. The results revealed an intercalated structure in ABS/OMT nanocomposites and the OMT layers mainly distribute in SAN phase. However, a completely exfoliated structure was found in ABS/BER–AO/OMT nanocomposites and OMT layers preferentially located in the BER phase which indicated that the OMT platelets had a much higher affinity with brominated epoxy resin than ABS resin. Based on the above morphological results, a schematic diagram of the ABS/OMT, ABS/BER–AO/OMT nanocomposites was established. The thermal degradation behavior was characterized by thermogravimetry. The results showed that the exfoliation of OMT can enhance the thermal stability of pure ABS resin and ABS/BER blends. An increase in the limited oxygen index (LOI) value was observed with the addition of OMT and it was found that such an enhancement is closely related to the morphologies of the chars formed after combustion. A synergistic effect between OMT and BER–AO during the combustion of the nanocomposites was found and a schematic mechanism was presented.

© 2006 Elsevier Ltd. All rights reserved.

*Keywords:* Acrylonitrile–butadiene–styrene; Brominated epoxy resin; Organo montmorillonite; Nanocomposites; Thermal degradation

## 1. Introduction

Acrylonitrile–butadiene–styrene (ABS) is a widely used thermoplastic material due to its good mechanical properties, chemical resistance and easy processing characteristics. ABS is composed of a styrene–acrylonitrile copolymer (SAN) matrix phase, with grafted polybutadiene particles whose composition, shape and size are complex and vary from product to product. One of the main drawbacks of ABS is its inherent flammability. Brominated epoxy resin (BER) is a high molecular weight polymeric flame retardant designed for a broad range of thermoplastic applications and used in ABS and PC/ABS blends with antimony oxide as a synergist. The polymeric nature

of BER and its chemical structure offer many advantages including high thermal stability and thermal aging, excellent processability, high UV stability and non-corrosive, etc. ABS/BER–AO composites are of significant commercial importance and widely applied in many electronic fields.

Polymer/layered silicate nanocomposites (PLSNs) are a new class of materials which have attracted much attention from both scientists and engineers in recent years due to their excellent properties such as high dimensional stability, heat deformation temperature, gas barrier performance, flame retardancy, and enhanced mechanical properties when compared with pure polymer materials or conventional composites (micro- and macro-composites) [1–7]. The properties of ABS/clay nanocomposites prepared in different ways including melt-processing, emulsion and in situ polymerization have been reported [8–12]. However, few work has been carried on the nanocomposites based on ABS/BER–AO flame

\* Corresponding author. Tel./fax: +86 571 87953712.

E-mail address: [zpfang@zju.edu.cn](mailto:zpfang@zju.edu.cn) (Z. Fang).

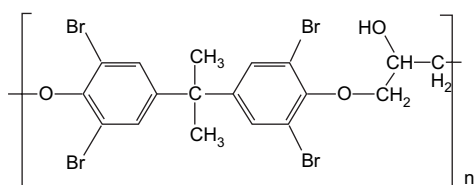
retarded systems. It is thought that ABS/BER–AO/clay nanocomposites may lead to a new kind of material with better heat performance and flame retardant properties, which combines the advantages of BER and the merits of clay which has excellent barrier properties.

In this work, ABS/clay and ABS/BER–AO/clay nanocomposites were prepared via melt compounding. The dispersion and intercalation/exfoliation of organoclay in nanocomposites were investigated by X-ray diffraction and transmission electron microscopy, based on which the preferential distribution model of clay in the nanocomposites was established. The thermal stability of the nanocomposites was measured by thermogravimetric analysis, and the degradation mechanism of nanocomposites was discussed. The fire retardancy was measured using limiting oxygen index (LOI). Studies on the char residue after LOI tests were performed using a Field Emission Scanning electron microscopy.

## 2. Experimental

### 2.1. Materials

The organically modified clay (Na<sup>+</sup>-montmorillonite) was supplied by Zhejiang Huate Clay Products of China, which was ion-exchanged with octadecyl trimethyl ammonium bromide (C<sub>18</sub>). The ABS resin (HI-121H) was obtained from LG Industries, Korea. Brominated epoxy resin (F-2100H showing in the following scheme) was purchased from ICL Industrial Products, the molecular weight is  $2.5 \times 10^4$ , the density is 1.8 g/cm<sup>3</sup>, and the bromine content is 53.0%. Antimony oxide (AO,  $M_w = 292$ ) was supplied by Hunan Huachang Antimony Industrial Co. Ltd and had the particle sizes of 2.0–5.0 μm.



### 2.2. Preparation of ABS/clay and ABS/BER–AO/clay nanocomposites

The ABS/clay, ABS/BER–AO, ABS/BER–AO/OMT in different proportions were mechanically mixed and then extruded in a twin screw extruder (TE-35, L/D = 35:1, Nanjing, China) at a rotational speed of 360 rpm. The temperature profiles of the barrel were 180–190–195–195 °C from hopper to die for all the samples. The mixed samples were transferred to a mold, then pressed at 14 MPa, and successively cooled to room temperature while maintaining the pressure to obtain the composite sheets for further measurements. Before mixing, all the polymers and clay were dried in a vacuum oven at 80 °C for at least 12 h. Table 1 shows the sample identification and composition.

Table 1

The sample identification and composition

| Identification | Weight ratio |
|----------------|--------------|
| ABS            | ABS          |
| ABS/OMT        | 100/2        |
| ABS/BER–AO     | 100/12/4     |
| ABS/BER–AO/OMT | 100/12/4/2   |

### 2.3. Characterization

Wide-angle X-ray diffraction (WAXD) was used to examine the dispersion of clay in composites. WAXD was carried out by using a Rigaku X-ray generator (Cu K $\alpha$  radiation with  $\lambda = 1.54$  Å) at room temperature. The diffractograms were obtained at the scattering angles from 0.5° to 10°, at a scanning rate of 2°/min. The transmission electron micrograph was obtained with a JEM-1200EX electron microscope to examine the dispersion and intercalation states of clay in composites. The nanocomposite samples for TEM observation were ultrathin-sectioned using a microtome equipped with a diamond knife. The sections (200–300 nm) were cut from a piece of about  $1 \times 1$  mm<sup>2</sup>, and they were collected in a trough filled with water and placed on a 200 mesh copper grid.

Thermogravimetry analysis (TGA) experiments were done in a TA SDT Q600 thermal analyzer using a scanning rate of 10 °C/min under air, from 60 to 600 °C.

The fire retardancy was measured using limiting oxygen index (LOI). This method followed the ASTM D2863-77 procedure, using specimens of  $130 \times 6.5 \times 3.0$  mm. Studies on the char residue after LOI tests were performed using a Field Emission Scanning electron microscopy (FEI Sirion FESEM).

## 3. Results and discussion

### 3.1. The dispersion of clay in nanocomposites

XRD is usually used to characterize the basal spacings of clay in polymer/clay hybrids and therefore the dispersion of the clay in nanocomposites. Fig. 1 shows the WAXD profiles of OMT, ABS/OMT, ABS/BER–AO/OMT nanocomposites. The peaks correspond to the (001) plane reflections of the clays. The (001) diffraction of OMT was at  $2\theta = 2.40^\circ$ , corresponding to an interlayer spacing of 1.92 nm. For the ABS/OMT composites, the characteristic (001) peak of the clay was shifted to  $2\theta = 2.42^\circ$  (corresponding to a basal spacing of 3.65 nm), and shows 1.74 nm gallery height increase than that of OMT. The increased spacing indicates that some ABS molecular chains were intercalated between the clay galleries forming an intercalated structure. On the other hand, the WAXD did not show any clay diffraction peaks for the ABS/BER–AO/OMT nanocomposites, suggesting that the clay platelets were completely exfoliated in the matrix. It had been reported that completely exfoliated structure can be obtained in epoxy/clay nanocomposites [13–16]. The WAXD results indicate that the clay has a much higher affinity with brominated epoxy resin than ABS. Therefore, clay may

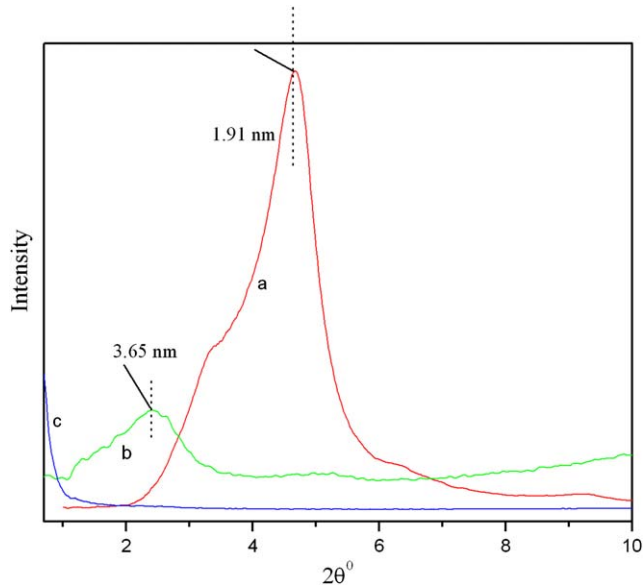


Fig. 1. WAXD profiles of the pristine OMT (a), ABS/OMT (b) and ABS/BER-AO/OMT (c) nanocomposites.

intercalate preferentially and selectively locate in the BER phase in the blend nanocomposites.

However, it is difficult for WXR D to draw definitive conclusions about the visualized dispersion of clay in nanocomposites. Thus, TEM techniques are necessary to characterize the morphology of the composites.

Fig. 2 shows TEM micrographs for the nanocomposites. In the ABS/OMT composites, the grey continuous region corresponds to SAN phase and the spherical rubber particles with different sizes spreading from 100 to 200 nm diameters appear as islands (Fig. 2A). The black lines correspond to clay platelets. The TEM micrograph for ABS/OMT nanocomposites shows that the clay layers consisted of multilayered stacks, about 20–50 nm in composites and clay mainly dispersed in SAN phase (the grey continuous region) (Fig. 2B). No serious agglomeration and individual silicate layers were seen in the composites and it indicates that no exfoliation occurred in the composites. On the other hand, in the micrographs of ABS/BER-AO/OMT nanocomposites, the region with scattered grey rubber particles is ABS phase (Fig. 2C) and the smooth region with more clay platelets is BER phase (Fig. 2D). Only a few discernible clay layers can be seen in

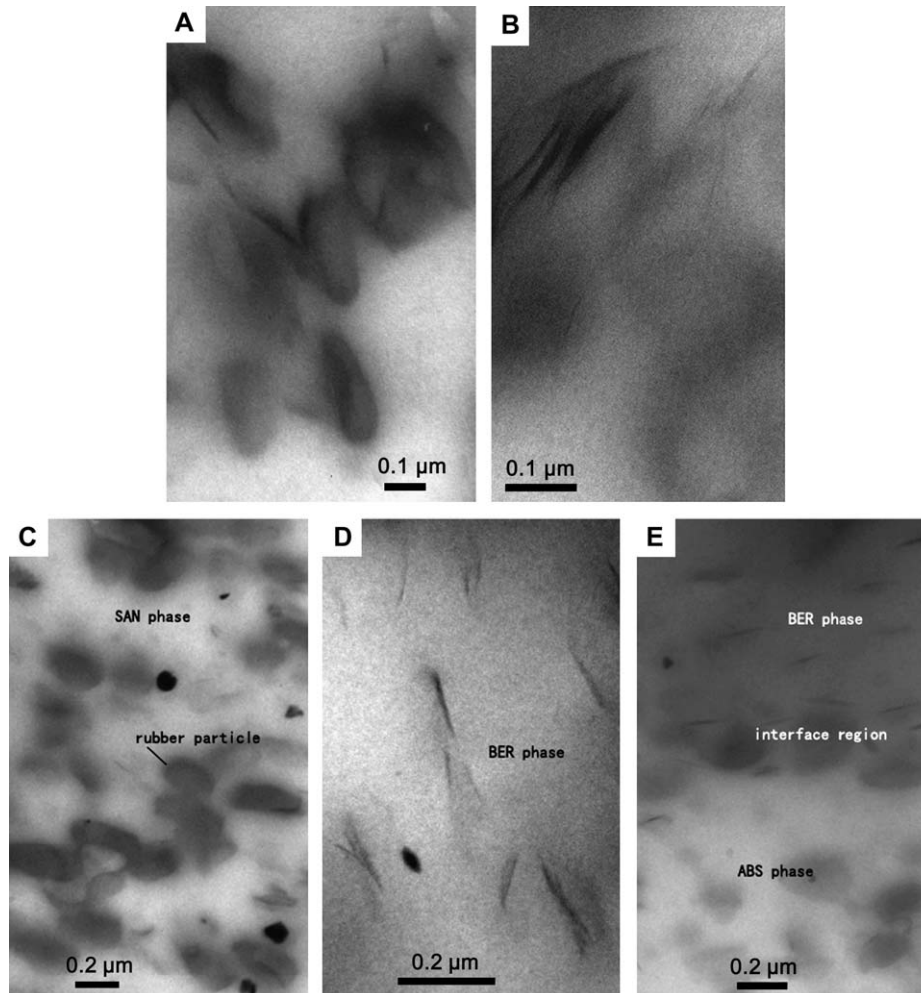


Fig. 2. TEM micrographs for ABS/OMT (A and B) and ABS/BER-AO/OMT (C, D and E) nanocomposites.

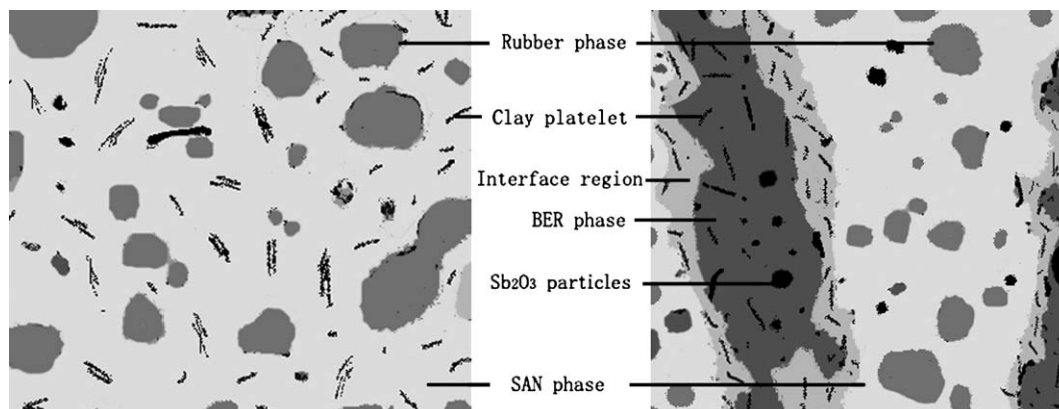


Fig. 3. Schematic diagram of the ABS/OMT (A) and ABS/BER–AO/OMT (B) nanocomposites.

the ABS phase in Fig. 2C, much less than that in BER phase, and the higher magnification TEM image (Fig. 2D) displays clearly the distribution of the clay platelets. The organoclay is well-dispersed and highly exfoliated into single platelets and is selectively located in the BER phase. Moreover, inter-phase region (Fig. 2E) between ABS and BER is obvious in which a higher density of dispersed organoclay layers is observed compared to the integral dispersion in the composites. The preferential intercalation of the clay in BER phase is due to the differential polarity between ABS and BER. The higher polarity of the BER chains than ABS results in stronger affinities between the organoclay and BER. All the TEM results are consistent with the WXRd data shown in Fig. 1.

Based on the morphological results obtained from TEM, a schematic diagram of the ABS/OMT, ABS/BER–AO/OMT nanocomposites is given in Fig. 3. It was expected that the exfoliated structure of organoclay in BER can improve the properties particularly enhance the thermal stability of the nanocomposites due to its excellent barrier properties.

### 3.2. Thermal analysis

The thermal stability of ABS/BER–AO/OMT hybrids was discussed and compared to that of pure ABS, ABS/OMT and ABS/BER systems. Typical TGA and DTG thermograms in air are shown in Figs. 4 and 5. Tables 2 and 3 summarize the TGA and DTG data for thermograms corresponded to Figs. 4 and 5, respectively. The results show that two steps of degradation, one around 300–500 °C and the other greater than 500 °C exist in pure ABS resin and ABS/OMT nanocomposites in complete agreement with the results obtained by Wang et al. [10]. ABS/OMT nanocomposites have a lower  $T_{\text{onset}}$  than pure ABS resin, which is attributed to thermal decomposition of organic modifiers of the clay. ABS/OMT nanocomposites have a higher  $T_{50\%}$  temperature and a larger residue showing an enhanced thermal stability due to the barrier properties of clay layers. The DTG results show a higher temperature at maximum degradation rate and a lower maximum degradation rate in ABS/OMT than that in pure ABS resin.

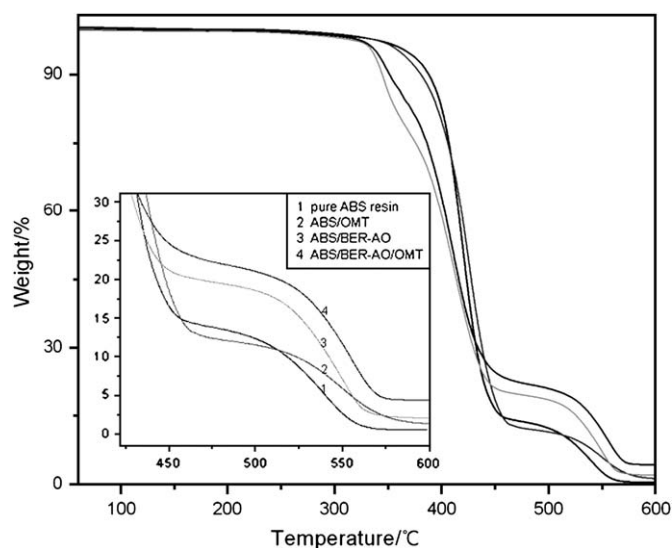


Fig. 4. TGA thermograms of ABS, ABS/OMT, ABS/BER–AO, ABS/BER–AO/OMT nanocomposites in air.

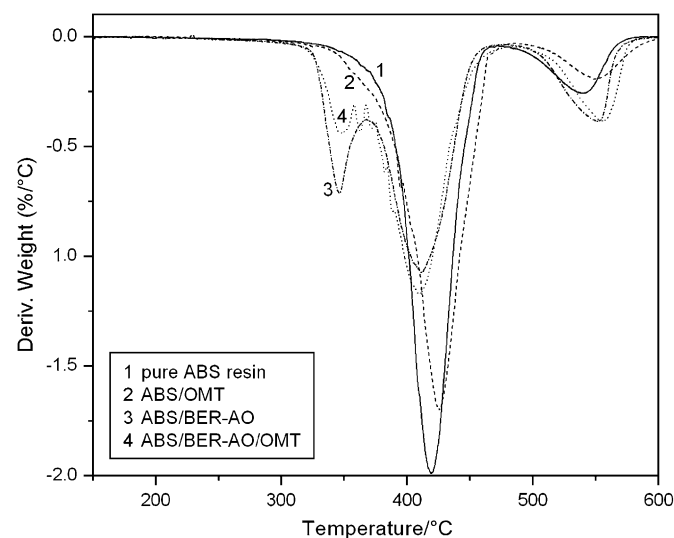


Fig. 5. DTG thermograms of ABS, ABS/OMT, ABS/BER–AO, ABS/BER–AO/OMT nanocomposites in air.



Table 2  
Data from thermal degradation analysis

|                | $T_{\text{onset}}$ | $T_{50\%}/^{\circ}\text{C}$ | Residue at 600 °C (wt%) |
|----------------|--------------------|-----------------------------|-------------------------|
| ABS            | 368.2              | 420.9                       | 0.55                    |
| ABS/OMT        | 361.1              | 424.4                       | 1.29                    |
| ABS/BER-AO     | 335.5              | 408.8                       | 2.06                    |
| ABS/BER-AO/OMT | 339.3              | 411.4                       | 3.62 <sup>a</sup>       |

$T_{\text{onset}}$ : 5% weight loss temperature (°C);  $T_{50\%}$ : 50% weight loss temperature (°C).

<sup>a</sup> The char for OMT over 60–600 °C has been subtracted.

The thermal degradation of ABS/BER and ABS/BER–AO/OMT consists of three independent steps. In the first step the  $T_{\text{onset}}$  of ABS/BER is about 335.5 °C, much lower than that of pure ABS resin, which can be assigned to the pyrolysis of BER. Isomerization of epoxy group, formation of hydrogen bromide (HBr) and the reactions between HBr and AO all occur in the first step. The second step can be considered as the thermal degradation of ABS resin which occurs from 350 to 500 °C. The degradation of the protective char residue occurs during the third step. The  $T_{\text{onset}}$ ,  $T_{50\%}$  in ABS/BER–AO/OMT nanocomposites are higher than that in ABS/BER–AO composites. The temperature at maximum degradation rate is increased and maximum degradation rate is reduced in different extent in the first steps. The char yield at 600 °C in ABS/BER–AO/OMT nanocomposites is 1.56 wt% higher than that of ABS/BER system in the condition that OMT over 60–600 °C has been subtracted. The results above indicate that the addition of organoclay enhances the thermal stability of the materials.

### 3.3. Flammability properties

The LOI test results are shown in Table 4. It is noted that LOI value of ABS/OMT is 0.6 slightly higher than that of pure ABS resin but the LOI value of ABS/BER–AO/OMT nanocomposites is 2.2 higher than that of ABS/BER–AO composites. The results indicated that synergistic effect does exist between BER–AO and organoclay in the combustion.

In an attempt to elucidate the enhancement of flame retardancy by organic clay and BER–AO, the morphologies of four different formulations after LOI testing were examined by digital camera and FESEM and the results are presented in Figs. 6 and 7, respectively. The results from Fig. 6 showed that the char of pure ABS resin was almost burnt out and the char of ABS/BER–AO composites was inhomogeneous, which can

Table 3  
DTG data for the thermal degradation of experiments

|                | First step       |                  | Second step      |                  | Third step       |                  |
|----------------|------------------|------------------|------------------|------------------|------------------|------------------|
|                | $T_{\text{max}}$ | $R_{\text{max}}$ | $T_{\text{max}}$ | $R_{\text{max}}$ | $T_{\text{max}}$ | $R_{\text{max}}$ |
| ABS            | –                | –                | 418.3            | 2.08             | 539.9            | 0.26             |
| ABS/OMT        | –                | –                | 426.7            | 1.76             | 549.3            | 0.21             |
| ABS/BER–AO     | 345.3            | 0.72             | 410.7            | 1.11             | 552.8            | 0.40             |
| ABS/BER–AO/OMT | 348.7            | 0.44             | 409.7            | 1.20             | 557.4            | 0.39             |

$T_{\text{max}}$ : temperature at maximum degradation rate;  $R_{\text{max}}$ : maximum degradation rate.

Table 4  
Results from LOI measurements

|                | LOI  |
|----------------|------|
| ABS            | 19.1 |
| ABS/OMT        | 20.5 |
| ABS/BER–AO     | 29.2 |
| ABS/BER–AO/OMT | 31.4 |

be due to the low compatibility between ABS and BER–AO. While an integrated char structure with relatively smooth surface was formed in the ABS/OMT and ABS/BER–AO/OMT nanocomposites. Such a structure has better barrier resistance to the evolution of flammable volatiles to the vapor phase and the oxygen ingress to the condensed phase. A spatially thicker and more uniform char was formed on the surface of ABS/BER–AO/OMT than that of ABS/OMT nanocomposites which indicated that synergistic effect exist between OMT and BER–AO.

The results from Fig. 7 showed detailed micromorphologies of the four different samples. The char of ABS/BER–AO composites was loose and porous which can be attributed to the expansion and permeation of vapor phase of BER–AO in the process of combustion. The chars of ABS/OMT and ABS/BER–AO/OMT nanocomposites were tighter and more dense than other residues, at the same time, the char residue of ABS/BER–AO/OMT was more dense, integrated and had fewer surface microcracks than that of ABS/OMT nanocomposites. The clay dispersion of the char residue after burning was presented in high magnification image (Fig. 7E,F). The clay layers can be clearly seen dispersed in the matrix and the association between clay layers and matrix is closer and tighter in ABS/BER–AO/OMT nanocomposites which can be attributed to the higher affinity between clay layers and BER than ABS resin. The results indicated that synergistic effect does exist between organic clay and BER and the ABS/BER–AO/OMT nanocomposites can lead to the formation of ceramic-like material with a homogeneous surface which will protect the material throughout combustion and also to a mechanical reinforcement of the charred layer which would lead to a better accommodation of strains.

### 3.4. Mechanism of the synergistic effect

The enhancement on thermal stability and flammability of ABS/BER–AO/OMT nanocomposites can be attribute to the good barrier properties and protective effect of organoclay which can isolate the underlying materials and lower down the mass loss rate of decomposition products. It is known that BER is a kind of gaseous flame retardant. The barrier effect of organoclay can be considered in two aspects. On one hand, the clay layers can delay the pyrolysis of BER and the reactions between BER and AO which occur at a relatively low temperature. Thus BER can maintain a continuous gaseous flame retarded effect. On the other hand, the synergistic effect exists between OMT and BER–AO. When OMT and BER–AO both are present, reactions occur [17,18] among

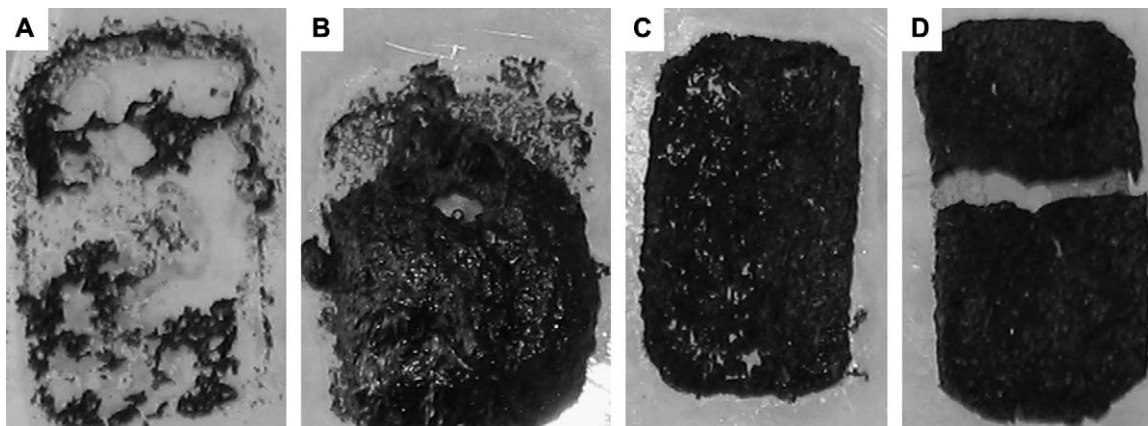


Fig. 6. Digital photographs of the chars formed after combustion (A) pure ABS resin, (B) ABS/BER-AO, (C) ABS/OMT, (D) ABS/BER-AO/OMT.

these compounds. The thermal degradation of  $C_{18}$  treated MMT takes place with Hoffmann elimination reaction [19].  $C_{18}$  are lamellar ionic crystals consisting alternating layers of paraffinic alkyl chains and of ionic groups and associated water of hydration. Upon degradation around 200 °C, the

entire structure is rapidly destroyed and yields fragments including long chain tertiary amines, long chain  $\alpha$ -olefins and 1-chloroalkanes, leaving an acid site ( $LS^-H^+$ ) on the surface of the MMT layers. The volatilization of fragments can expand the clay layers and enlarge the basal spacing. Moreover,

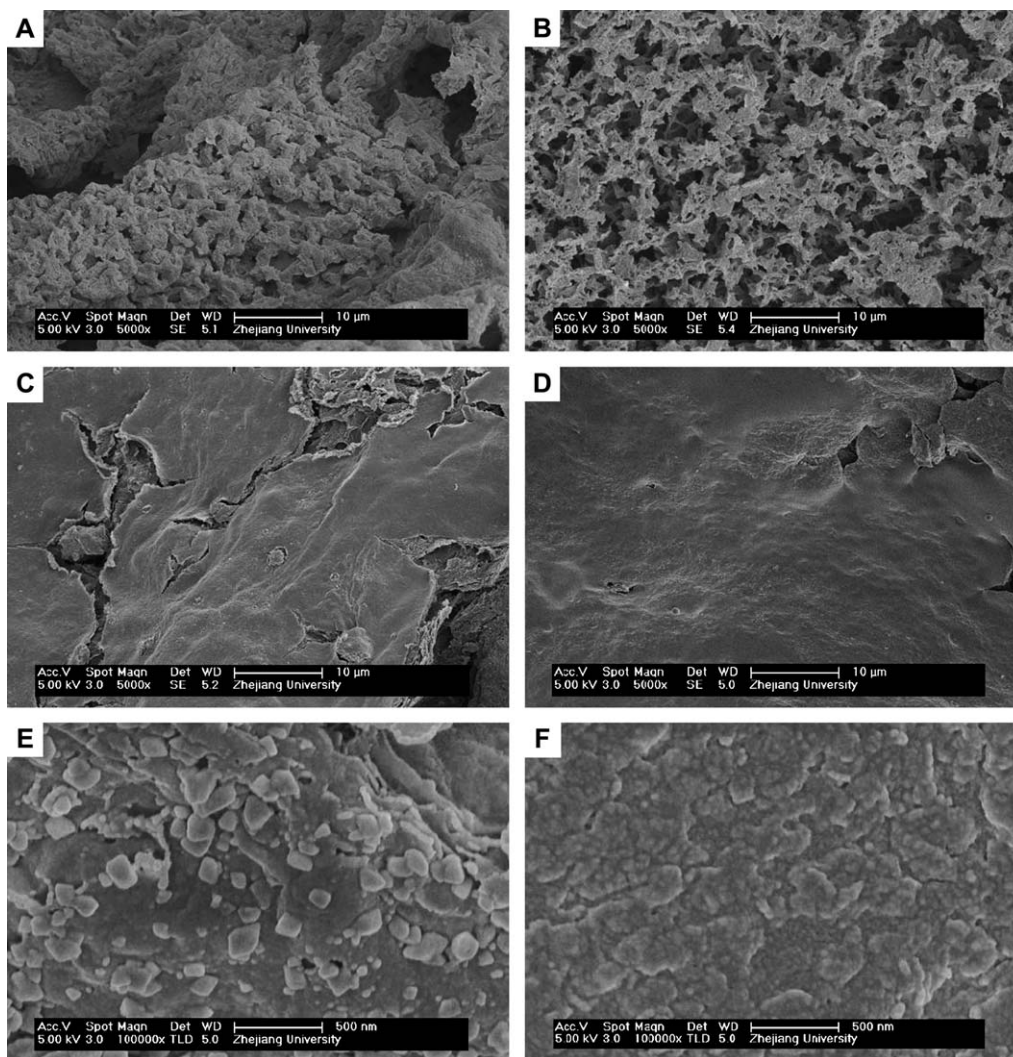


Fig. 7. FESEM micrographs of the chars formed after LOI test (A) pure ABS resin, (B) ABS/BER-AO, (C, E) ABS/OMT, (D, F) ABS/BER-AO/OMT.

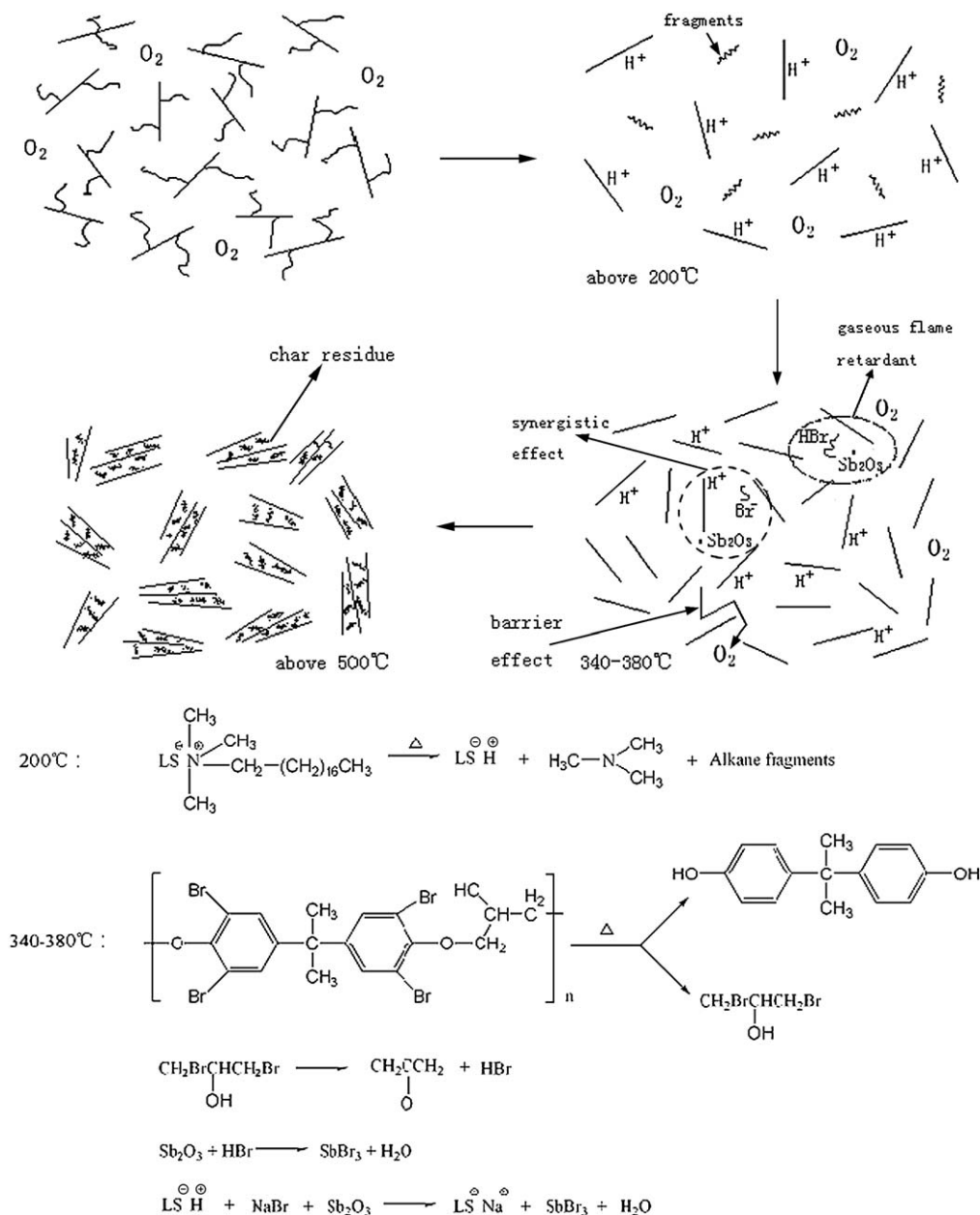


Fig. 8. Schematic representation of combustion mechanism and the synergistic effect between OMT and BER–AO nanocomposites.

exfoliated nanocomposites have better barrier properties and thermal stability than intercalated ones [20,21]. At a higher temperature (about 330–350 °C) the degradation of BER yields gaseous HBr which can react with antimony oxide.  $\text{LS}^- \text{H}^+$ , AO and sodium bromide which appears due to the cation exchange montmorillonite react and yield antimony tri-bromide, a well-known substance for flame retarding. Schematic representation of combustion mechanism and the synergistic effect between OMT and BER–AO nanocomposites are shown in Fig. 8.

#### 4. Conclusions

The clay shows an intercalated structure in ABS/OMT nanocomposites and mainly distributed in SAN phase.

However, a completely exfoliated structure formed in ABS/BER–AO/OMT nanocomposites and the clay layers intercalate preferentially and selectively locate in the BER phase which indicates that the clay platelets have a much higher affinity with brominated epoxy resin than with ABS resin due to the higher polarity of the BER chains.

The thermal degradation results showed that the exfoliation of clay can enhance the thermal stability of pure ABS resin and ABS/BER blends. An increase in the limited oxygen index (LOI) value was observed with the addition of organoclay and it was also found that the enhancement is closely related to the morphologies of the chars formed after combustion. A synergistic effect exists between OMT and BER–AO. The temperature at maximum degradation rate is increased and the maximum degradation rate is reduced in different extents.

**References**

- [1] Jin Z, Morgan AB, Lamelas FJ, Wilkie CA. *Chem Mater* 2001;13:3774–80.
- [2] Haradwaj RK. *Macromolecules* 2001;34:9189–92.
- [3] Robello DR, Yamaguchi N, Blanton T, Barnes C. *J Am Chem Soc* 2004;126:8118–9.
- [4] Su SP, Jiang DD, Wilkie CA. *Polym Degrad Stab* 2004;84:279–88.
- [5] Ramos Filho FG, Melo TJA, Rabello MS, Silva SML. *Polym Degrad Stab* 2005;89:383–92.
- [6] Shah D, Maiti P, Jiang DD, Batt CA, Giannelis EP. *Adv Mater* 2005;17:525–6.
- [7] Zheng XX, Wilkie CA. *Polym Degrad Stab* 2003;82:441–50.
- [8] Choi YS, Xu MZ, Chung IJ. *Polymer* 2005;46:531–8.
- [9] Stretz HA, Paul DR, Casidy PE. *Polymer* 2005;46:3818–30.
- [10] Wang SF, Hu Y, Lei S, Wang ZZ, Chen ZY, Fan WC. *Polym Degrad Stab* 2002;77:423–6.
- [11] Wang SF, Hu Y, Zong RW, Tang Y, Chen ZY, Fan WC. *Appl Clay Sci* 2004;25:49–55.
- [12] Pourabas B, Raeesi V. *Polymer* 2005;46:5533–40.
- [13] Gu AJ, Liang GZ. *Polym Degrad Stab* 2003;80:383–91.
- [14] Zhang KL, Wang LX, Wang F, Wang GJ, Li ZB. *J Appl Polym Sci* 2004;91:2649–52.
- [15] Chen B, Liu J, Chen HB, Wu JS. *Chem Mater* 2004;16:4864–6.
- [16] Jan IN, Lee TM, Chiou KC, Lin JJ. *Ind Eng Chem Res* 2005;44:2086–90.
- [17] Zanetti M, Gao ZM, Pan WP, Hunter D, Singh A, Vaia R. *Chem Mater* 2002;14:881–7.
- [18] Zanetti M, Camino G, Peter R, Mulhaupt R. *Chem Mater* 2002;14:189–93.
- [19] Xie W, Gao ZM, Pan WP, Hunter D, Singh A, Vaia R. *Chem Mater* 2001;13:2979–90.
- [20] Lebaron PC, Wang Z, Pinnavaia TJ. *Appl Clay Sci* 1999;15:11–29.
- [21] Pinnavaia TJ, Beall GW. *Polymer–clay nanocomposites*. Chichester/New York: Wiley; 2000.